International Journal of Thermophysics, Vol. 28, No. 2, April 2007 (© 2007)
DOI: 10.1007/s10765-007-0154-6

Solvation Structure of Ions in Water

Raymond D. Mountain[1]

Molecular dynamics simulations of ions in water are reported for solutions of varying solute concentration at ambient conditions for six cations and four anions in 10 solutes. The solutes were selected to show trends in properties as the size and charge density of the ions change. The emphasis is on how the structure of water is modified by the presence of the ions and how many water molecules are present in the first solvation shell of the ions.

KEY WORDS: anion; cation; molecular dynamics; potential functions; solvation; water.

1. INTRODUCTION

The behavior of aqueous solutions of salts is a topic of continuing interest [1–3]. In this note we examine how the structure of water, as reflected in the oxygen–oxygen pair function, is modified as the concentration of ions increases. The method of generating the pair functions is molecular dynamics using the SPC/E model for water [4] and various models for ion–water interactions taken from the literature. The solutes are LiCl, NaCl, KCl, RbCl, NaF, $CaCl_2$, $CaSO_4$, Na_2SO_4, $NaNO_3$, and guanidinium chloride (GdmCl) [$C(NH_2)_3Cl$]. This work is an extension of earlier work [5] to a larger set of ions.

The water molecules and ions interact through site–site pair interactions consisting of Lennard–Jones potentials and Coulomb interactions so that the interaction between a pair of sites labeled i, j and separated by an interatomic distance r is

$$\phi_{ij}(r) = 4\epsilon_{ij}\left[(\sigma_{ij}/r)^{12} - (\sigma_{ij}/r)^{6}\right] + q_i q_j / r \tag{1}$$

where q_i is the charge on site i.

[1] Physical and Chemical Properties Division, Chemical Science and Technology Laboratory, National Institute of Standards and Technology, Gaithersburg, Maryland 20899-8380, U.S.A. E-mail: rmountain@nist.gov

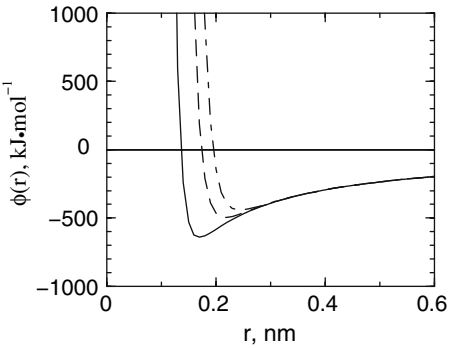

Fig. 1. Ion–oxygen pair potentials for Na^+ (solid line), K^+ (dashed line), and Rb^+ (long-short dashed line) are shown here.

The various potential parameters used here are listed in Table I. The parameters ϵ and σ for unlike sites are determined using the Lorentz–Berthelot combining rules [12]. The results for the potential models used here should be considered as providing a qualitative view of what happens in aqueous solutions but should not be assumed to be quantitatively accurate.

Figure 1 shows some of the ion–water pair potentials. The balance between the Coulomb and r^{-12} terms leads to effective well depths that are much larger than the ϵ parameters. Note that the Coulomb contribution overwhelms the Lennard-Jones contribution for separations larger than about 0.4 nm. Similar potentials are obtained for the other ion sites.

The simulations have a total number of molecules (water plus ions) of 216 except for the GdmCl solute where 1000 particles were used. The size of the Gdm^+ ion calls for a large system so that the spatial correlations do not exceed the simulation cell size. The individual ions are considered to be distinct entities when determining mole fractions. The equations of motion are integrated using the Beeman algorithm [13, 14] with a time step of 1 fs. Water and the molecular ions are treated as rigid objects with the orientations described by quaternions [15–17]. The Ewald summation method is used to treat the long-range part of the Coulomb interaction [18, 19]. The Lennard-Jones interactions were truncated at 1/2 the simulation cell edge length. For each composition examined, the volume of the cubic simulation cell was adjusted so that the computed pressure was close to ambient pressure at the system temperature of 293 K. For each case, an equilibration run of 100 ps was made to ensure that the pressure was satisfactory. Then a production run of at least 100 ps was

Table I. Interaction Parameters (Geometry of the molecules is found in the listed references.)

Solute	ϵ (kJ·mol^{-1})	σ (nm)	q (e)	References
LiCl				
Li	0.558	0.139	1	[6]
Cl	3.484	0.393	−1	[6]
NaF				
Na	0.482	0.227	1	[6]
F	2.230	0.273	−1	[6]
NaCl				
Na	0.407	0.221	1	[7]
Cl	0.493	0.442	−1	[7]
KCl				
K	0.001	0.474	1	[7]
Cl	0.493	0.442	−1	[7]
RbCl				
Rb	0.001	0.527	1	[7]
Cl	0.442	0.442	−1	[7]
$CaCl_2$				
Ca	1.886	0.236	2	[7]
Cl	0.493	0.442	−1	[7]
Na_2SO_4				
Na	0.407	0.221	1	[7]
S	1.046	0.355	2	[8]
O	0.837	0.315	−1	[8]
$CaSO_4$				
Ca	1.886	0.236	2	[7]
S	1.046	0.355	2	[8]
O	0.837	0.315	−1	[8]
$NaNO_3$				
Na	0.194	0.399	1	[9]
N	0.865	0.283	0.95	[9]
O	1.798	0.256	−0.65	[9]
GdmCl				
C	0.417	0.377	1	[10]
N	0.500	0.311	−0.8	[10]
H	0.088	0.158	0.4	[10]
Cl	0.470	0.440	−1	[11]
H_2O				
O	0.651	0.3166	−0.8476	[4]
H	0	–	0.4238	[4]

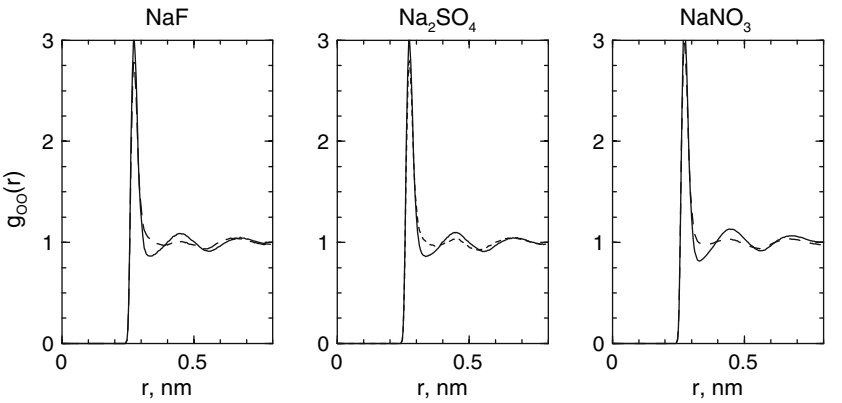

Fig. 2. Oxygen–oxygen pair functions in the presence of increasing ionic concentration are shown here. For NaF, the mole fractions of water are 0.991 (solid line) and 0.963 (dashed line). For Na_2SO_4 the mole fractions of water are 0.986 (solid line) and 0.944 (dashed line). For $NaNO_3$ the mole fractions of water are 0.991 (solid line) and 0.889 (dashed line).

made. If the lifetime of water molecules in the first solvation shell was more than about 20 ps, longer production runs were made.

An indication of how the structure of water is changed as the solute concentration increases is shown in Fig. 2. There the oxygen–oxygen pair functions for the solutes NaF, Na_2SO_4, and $NaNO_3$ are displayed for two concentrations as stated in the figure caption. Similar results, with details that depend on the shape of the ions and on the particular potential parameters, were obtained, but not shown here, for other solutes listed in Table I. The loss of structure of the second maximum in the pair function, at a separation r_2, indicates that the tetrahedral structure of water is disrupted as the concentration of ions increases. The main difference between the various solutes is in how much solute is needed to supress the second maximum. A quantative indicator of "how much" is discussed in the next section.

2. SOLVATION STRUCTURE

The first solvation shell of an ion consists of those water molecules that are within a region determined by the position of the first minimum of the cation-oxygen site correlation function (R_+) or of the anion-hydrogen site correlation function (R_-) as illustrated in Fig. 3. The number and variance of the water molecules in the first solvation shell provide an indication of the solvation structure.

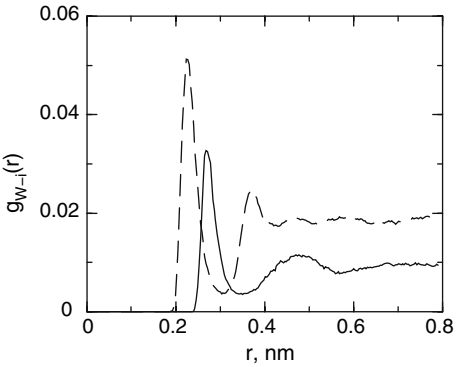

Fig. 3. Ion water pair functions determine the size of the first solvation shell taken to be the position of the minimum. This case is for KCl. Solid line is the oxygen–K pair function, and dashed line is the hydrogen–Cl pair function. Water mole fraction is 0.99. K solvation shell radius, R_+, is 0.357 nm, and Cl shell radius, R_-, is 0.303 nm.

A summary of the occupation numbers of the first solvation shell is contained in Table II. The systems were sampled at an interval of 0.1 ps, and the number of water molecules within the solvation shell were counted. The average and variance of the number of molecules are based on 1000 samples. An ion with a high charge density, such as Li^+, has a small variance in the number of water molecules in the first shell while larger ions, such as sulfate and nitrate, have large variances.

The numbers for molecular ions need some additional comment. For the sulfate and nitrate ions the results are for the solvation of the anion O-sites by the H-sites on water and the distances listed are not from the center of mass. The same observation applies to the Gdm^+ ion where the distance is between the outer H-sites of the ion and the O-site of water.

For all of the cases examined, the number of water molecules solvating the ions is roughly proportional to the number of ions present. This indicates that the incidence of water molecules solvating more than one ion is low and that there is relatively little ion pairing. No constraints on the separation of the ions were imposed during the simulations.

Recently it was demonstrated that the changes in water structure associated with the addition of salt were similar to those that occur with the application of pressure in the order of 100 MPa [20]. For most of the solutes examined, the volume of the simulation cell decreased with decreasing

Table II. Solvation Ranges (R_+, R_-) and Number of Waters in the First Solvation Shell (N_+, N_-) are Listed for the Solutes.

Solute	R_+ (nm)	N_+	R_- (nm)	N_-
NaCl	0.329	5.72 (0.49)	0.278	6.53 (0.86)
KCl	0.357	5.38 (1.12)	0.275	5.31 (1.07)
RbCl	0.357	5.50 (1.03)	0.275	5.18 (0.93)
LiCl	0.316	4.07 (0.27)	0.278	6.68 (0.87)
NaF	0.329	5.86 (0.46)	0.278	6.54 (0.57)
$CaCl_2$	0.325	7.96 (0.20)	0.281	6.40 (1.28)
$CaSO_4$	0.335	6.75 (0.82)	0.240	11.30 (1.46)
Na_2SO_4	0.357	5.80 (0.69)	0.228	12.70 (0.72)
$NaNO_3$	0.348	6.74 (0.90)	0.215	5.14 (1.33)
GdmCl	0.243	5.33 (0.87)	0.277	6.86 (0.63)

Numbers in parentheses are the variances of the number of solvating water molecules. For molecular ions, the distance listed is measured from the water site to the outermost site on the ion.

mole fraction of water (increased solute concentration). The exceptions are $NaNO_3$ and GdmCl. This is indicated in Fig. 4 where the ratio of the volume of the system with water mole fraction X_W to the volume of the system with zero solute is shown as a function of X_W. The mole fraction of water is the ratio of the number of water molecules to the total number of water molecules plus cations plus anions. The NO_3^- and Gdm^+ ions are large, planar objects with distributed charges and therefore have a smaller contractive effect on the surrounding water molecules.

Figure 2 indicates that the amount of solute needed to significantly reduce the local structure of water, as indicated by the magnitude of the second maximum in $g_{OO}(r)$, depends on the ions in the solute. In Fig. 5, we show how the magnitude of the second maximum is reduced as the mole fraction of the water is reduced. There the magnitude of the second maximum, at postion r_2, is shown for the solutes considered in this work. This figure suggests that the solutes can be ordered in terms of the efficiency of disruption, starting with the most efficient disrupter of local structure in the water, as NaF, LiCl, NaCl, KCl, RbCl, $CaCl_2$, $CaSO_4$, Na_2SO_4, $NaNO_3$, and GdmCl.

3. CONCLUSION

The simulation results show that the amount of disruption of the second neighbor signature of tetrahedral order in water for a given mole fraction of water increases with the charge density of the ions. This is the case

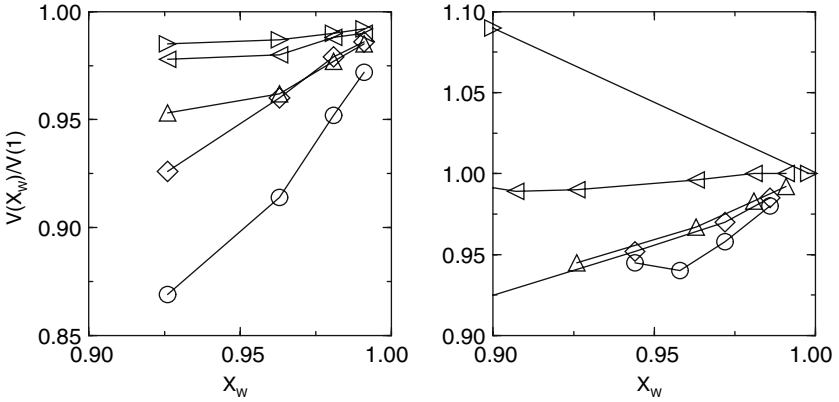

Fig. 4. Volume ratio of the system containing solute to the volume with zero solute is shown as a function of the mole fraction of water. In the left-side panel, the symbols indicate the following solutes: ◯, NaF; ◇, LiCl; △, NaCl; ◁, KCl; ▷, RbCl. In the right-side panel, the symbols indicate the following solutes: ◯, $CaCl_2$; △, $CaSO_4$; ◇, Na_2SO_4; ◁, $NaNO_3$, ▷, GdmCl.

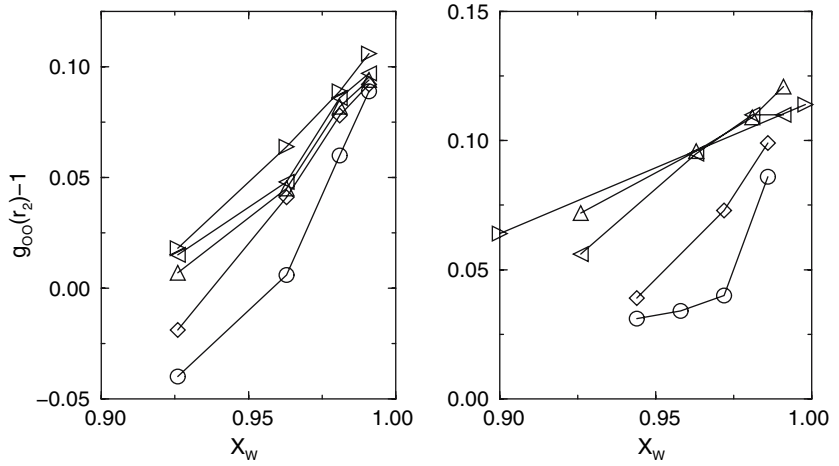

Fig. 5. Reduction in the height of the second maximum in the oxygen–oxygen pair function, normalized to unity for large r, is shown as a function of the mole fraction of water. The second maximum is at r_2. In the left-side panel, the symbols indicate the following solutes: ◯, NaF; ◇, LiCl; △, NaCl; ◁, KCl; ▷, RbCl. In the right-side panel, the symbols indicate the following solutes: ◯, $CaCl_2$; △, $CaSO_4$; ◇, Na_2SO_4; ◁, $NaNO_3$, ▷, GdmCl.

for metal cations and for Cl^- and F^-. It also occurs for the molecular ions SO_4^{2-}, NO_3^-, and Gdm^+. This is reflected in the sequence of solutes listed at the end of Section 2. The change in the volume of the fluid shown in Fig. 4, which follows the sequence of disrupters, is a macroscopic indication of how the molecular level structure of water is modified as salt is added.

REFERENCES

1. E. Guàrdia, D. Laria, and J. Marti, *J. Phys. Chem. B* **110**:6332 (2006).
2. L.-A. Näslund, D. C. Edwards, P. Wernet, U. Bergmann, H. Ogasawara, L. G. M. Pettersson, S. Mynei, and A. Nilsson, *J. Phys. Chem. A* **109**:5995 (2005).
3. A. Wahab, S. Mahuiuddin, G. Hefter, W. Kunz, B. Minorar, and P. Jungwirth, *J. Phys. Chem. B* **109**:24108 (2005).
4. H. J. C. Berendsen, J. R. Grigera, and T. P. Straatsma, *J. Phys. Chem.* **91**:6269 (1987).
5. R. D. Mountain and D. Thirumalai, *J. Phys. Chem. B* **108**:19711 (2004).
6. B. M. Pettit and P. J. Rossky, *J. Chem. Phys.* **84**:5836 (1986).
7. P. B. Balbuena, K. P. Johnston, and P. J. Rossky, *J. Phys. Chem.* **100**:2706 (1996).
8. W. R. Cannon, B. M. Pettitt, and J. A. McCammon, *J. Phys. Chem.* **98**:6225 (1994).
9. R. M. Lyden-Bell, M. Ferario, and I. R. McDonald, *J. Phys.: Condens. Matter* **1**:6523 (1989).
10. S. Weerasinghe and P. E. Smith, *J. Chem. Phys.* **121**:2180 (2004).
11. S. Weerasinghe and P. E. Smith, *J. Chem. Phys.* **119**:11342 (2003).
12. J. P. Hansen and I. R. McDonald, *Theory of Simple Liquids* (Academic Press, New York, 1986,), p. 179.
13. P. Schofield, *Comput. Phys. Comm.* **5**:17 (1973).
14. D. Beeman, *J. Comput. Phys.* **20**:130 (1976).
15. D. J. Evans and S. Murad, *Mol. Phys.* **34**:327 (1977).
16. R. Sonnenschein, *J. Comput. Phys.* **59**:347 (1985).
17. D. C. Rapaport, *J. Comput. Phys.* **60**:306 (1985).
18. M. P. Allen and D. J. Tildesley, *Computer Simulation of Liquids* (Clarendon Press, Oxford, 1987), pp. 158–162.
19. D. Frenkel and B. Smit, *Understanding Molecular Simulation, from Algorithms to Applications*, 2nd Ed. (Academic Press, New York, 2002), pp. 292–300.
20. R. Leberman and A. K. Soper, *Nature* **378**:364 (1995).